Philosophical Magazine. Vol. 87. Núm. 27. 2007. Pag. 4151-4167
http://dx.doi.org/10.1080/14786430701530990

On the isothermal kinetics analysis of transformations in metastable systems. A combined use of isothermal and non-isothermal calorimetry.

(Short version: Isothermal analysis of transformation in metastable systems)

J. S. BLÁZQUEZ, M. MILLÁN, C. F. CONDE, A. CONDE*

Departamento de Física de la Materia Condensada. Universidad de Sevilla. Apartado 1065, 41080 Sevilla (Spain).

A procedure to optimize the isothermal calorimetric data of very slow transformation processes of metastable systems is proposed. The method uses an experimental baseline to identify the transitory effects due to the equipment. Moreover, the combined use of isothermal and non-isothermal results is shown to be effective to overcome the intrinsic problems of low signal and signal drift for such processes. The procedure has been applied to the analysis of the nanocrystallization kinetics of the $Fe_{60}Co_{18}Nb_6B_{16}$ alloy at different devitrification stages. Based on microstructural observations, an instantaneous growth approach was assumed and a phenomenological expression of the dependence of the nucleation frequency with both the transformed fraction and the temperature was obtained.

Keywords: crystallization; nanocrystalline microstructure; phase transformation kinetics.

*Corresponding author: Prof. A. Conde
Phone: (34) 95 455 28 85
Fax: (34) 95 461 20 97
E-mail: conde@us.es

Philosophical Magazine. Vol. 87. Núm. 27. 2007. Pag. 4151-4167
http://dx.doi.org/10.1080/14786430701530990

1. Introduction

Nowadays, metallic alloys in a metastable state, as amorphous, nanocrystalline, or quasicrystalline systems, are used in a wide spectrum of technological applications due to the improvement of physical (e. g. mechanical, magnetic) and chemical (e. g. corrosion resistance) properties with respect to those in a thermodynamically stable state (e.g. [1,2] and references therein). The study of the kinetics of the transformations producing or destroying such structures is, therefore, an important task in order to optimize these materials and to control their microstructure.

In the particular case of nanocrystalline alloys obtained by controlled crystallization of a precursor amorphous alloy, nanocrystallization is a primary crystallization process in which very small crystallites of phases rich in the main element of the composition (e. g. α-Fe in Fe based alloys [1], α-Al in Al based alloys [2]) are embedded in a residual amorphous matrix which is progressively enriched in the elements with low solubility in the crystalline phase. A common feature in these alloy compositions is the presence of elements enhancing the glass forming ability of the system, in order to achieve the precursor amorphous alloy (normally close to eutectics of binary alloys with the main element of the composition: Fe-B, Al-Ni), and other elements with very low diffusivity, which constraint the growth of the crystallites to a nanometric scale (Nb, Zr, Hf [1], Y, Lanthanides [2]). In some cases, small addition of some other elements has been shown to enhance the nucleation phenomenon, refining the nanocrystalline microstructure [3,4].

The nucleation and growth theories of crystallization are developed for isothermal conditions [5,6], although, as it will be shown later, some approaches can extend their validity to non-isothermal regimes. However, the use of isothermal records

Philosophical Magazine. Vol. 87. Núm. 27. 2007. Pag. 4151-4167
http://dx.doi.org/10.1080/14786430701530990
is always desired as the thermal dependence of several parameters can be ignored. In order to obtain the transformed fraction as a function of time at a constant temperature, it is possible to measure it from microstructural observations (X-ray diffraction, electron microscopy). However, the process must be stopped to acquire the data and results from several experiments must be combined. Therefore, in situ measurement, although indirect, are very suitable to study the transformation kinetics. Several experimental techniques have been used to follow in situ the devitrification process of amorphous alloys, among them: calorimetry (e.g. [7]), electrical resistivity measurements (e.g. [8]) or magnetization measurements when the forming phase is ferromagnetic (e.g. [9]). Calorimetric methods link the transformed fraction with the enthalpy developed in the process. However, nanocrystallization process is widely extended in time for isothermal experiments and, therefore, some problems arise inherent to the equipment stability for very long times as well as in the transient time affected by the way the isothermal regime is achieved. The aim of this work is to analyze these effects in order to optimize the reliability of the data extracted from isothermal transformations of metastable systems. The proposed procedure was applied to the nanocrystallization process of a $Fe_{60}Co_{18}Nb_6B_{16}$ amorphous alloy.

2. Theoretical models

Crystallization kinetics of metallic glasses is usually studied in the frame of the Johnson-Mehl-Avrami-Kolmogorov (JMAK) theory [10,11,12,13,14]. This theory supplies a relationship between the actual transformed volume fraction, $X(t)$, and the extended transformed volume fraction, $X^{ext}(t)$, which is the volume transformed without taking into account that one region already transformed can not be transformed again.

Philosophical Magazine. Vol. 87. Núm. 27. 2007. Pag. 4151-4167
http://dx.doi.org/10.1080/14786430701530990

The following expression, introduced by Johnson and Mehl [10], Avrami [11,12,13] and Kolmogorov [14], considers the probabilistic character of a certain volume of the sample to be suitable for transformation as the transformation progresses, the so-called geometrical effect [6,11,12,13,15].

$$\frac{dX}{dX^{ext}} = (1 - X) \tag{1}$$

In the simplest idea, the transformation involves the complete system and X would be 1 only if the whole volume of the sample is transformed (all the atoms in the system are suitable to transform into the configuration of the product phase(s)). However, we normalized X to the final value of the nanocrystallization process. At that stage, the sample is not fully transformed but some amount of residual amorphous matrix remains [16] as typically occurs in primary crystallization processes. This fact is characteristic of transformations in which the compositions of the product phase(s) and that of the parent phase(s) are not the same. In such cases, a compositional change of the parent phase(s) occurs during the transformation, due to an enrichment in elements non soluble in the product phase (α-Fe in the present study), and a soft impingement in the nucleation and growth processes is derived from the overlapping of the depleted regions generated by the product units during their growth. These facts yield the definition of two different regions in the untransformed phase [15], an inert space for the transformation, X^{inert}, which will remain untransformed at the end of the process, and an active space, X^{active}, suitable to be transformed. In this study, the normalization chosen for X (1 at the end of the nanocrystallization process) leads to assume implicitly the soft impingement due to the overlapping between Fe depleted regions, being $X^{inert} = 0$ [17]. In fact, the blocking of the growth of the nanocrystals can be ascribed to the pile up of atoms non-soluble in α-Fe grains and with a very slow diffusivity in the amorphous matrix [18], Nb in the studied alloy.

Philosophical Magazine. Vol. 87. Núm. 27. 2007. Pag. 4151-4167
http://dx.doi.org/10.1080/14786430701530990

Equation 1 can be modified to consider a stronger impingement than that only due to the geometrical effect considered in the JMAK theory [19].

$$\frac{dX}{dX^{ext}} = (1-X)^{2-\gamma} \tag{2}$$

where γ is the impingement factor. Other authors describe the same equation in terms of the impingement parameter $\eta = 1/(1-\gamma)$ [20]. In any case, the values of γ are between 0 and 1.

In the case of $\gamma = 1$, Eq. 1 is recovered and JMAK theory is applied. Considering the functional form of $X^{ext} = \left[K(T)\cdot\left(t-t_0\right)\right]^n$, the well known expression *X(t)* for JMAK theory is found:

$$X = 1-\exp\left[-\left\{K(T)\cdot\left(t-t_0\right)\right\}^n\right] \tag{3}$$

where *K(T)* is the frequency factor, *n* is the Avrami exponent, which can be obtained from the slope of the $\ln\left[-\ln\left(1-X\right)\right]$ vs. the $\ln\left(t-t_0\right)$ (JMAK plot) and t_0 is the induction time. A local value of the Avrami exponent, *n(X)*, can also be obtained for the isothermal regimes from:

$$n(x) = \frac{d\left(\ln\left[-\ln\left(1-X\right)\right]\right)}{d\left(\ln\left(t-t_0\right)\right)} \tag{4}$$

and for the non-isothermal regimes, taking into account the thermal dependence of *K(T)*, from [21]:

$$\frac{d\left(\ln\left[-\ln\left(1-X\right)\right]\right)}{d\left(\ln\left(\frac{T-T_o}{\beta}\right)\right)} = n(X)\left\{1+\frac{Q}{RT}\left(1-\frac{T_o}{T}\right)\right\} \tag{5}$$

where Q is the effective activation energy, R is the gas constant and T_o is the crystallization onset temperature.

In the general case of $\gamma \neq 1$, integration of Eq. 2 leads to:

Philosophical Magazine. Vol. 87. Núm. 27. 2007. Pag. 4151-4167
http://dx.doi.org/10.1080/14786430701530990

$$X = 1 - \frac{1}{\left[(1-\gamma)\left[K(T)\cdot(t-t_0)\right]^{n^*}+1\right]^{\frac{1}{1-\gamma}}} \tag{6}$$

which, for the limit value γ=0, yields the Austin-Rickett (AR) equation [22]:

$$X = 1 - \frac{1}{\left[K(T)\cdot(t-t_0)\right]^{n^*}+1} \tag{7}$$

In this equation the value of n^*, akin to the Avrami exponent, can be obtained from the slope of $\ln\left(\frac{1}{1-X}-1\right)$ vs. $\ln(t-t_0)$ (AR plot). Analogously to expression (4), a local value, $n^*(X)$, can be obtained for isothermal

$$n^*(X) = \frac{d\left(\ln\left[\frac{1}{1-X}-1\right]\right)}{d\left(\ln(t-t_0)\right)} \tag{8}$$

and non-isothermal regimes:

$$\frac{d\left(\ln\left[\frac{1}{1-X}-1\right]\right)}{d\left(\ln\left(\frac{T-T_o}{\beta}\right)\right)} = n^*(X)\left\{1+\frac{Q}{RT}\left(1-\frac{T}{T_o}\right)\right\} \tag{9}$$

in a similar way as it was done in [21] for the JMAK theory.

3. Experimental

Ribbons (5 mm wide and 20 μm thick) of $Fe_{60}Co_{18}Nb_6B_{16}$ alloy were produced by melt-spinning technique. Kinetics of the nanocrystallization process was studied from differential scanning calorimetry (DSC) experiments performed on a Perkin-Elmer DSC7 under argon flow. Pb and K_2CrO_4 standards were used to calibrate the equipment. Ribbon pieces were cut and placed into graphite pans. In order to reduce the factors

Philosophical Magazine. Vol. 87. Núm. 27. 2007. Pag. 4151-4167
http://dx.doi.org/10.1080/14786430701530990

affecting the DSC signal, a several-step procedure was followed without taking the sample out of the calorimeter:

- First, the sample was heated at 20 K/min up to the selected temperature for the isothermal treatment.
- Second, the sample was annealed during 5 h at this temperature.
- Third, the sample was cooled down to 323 K and stabilized.
- Fourth, a continuous heating at 20 K/min up to 1000 K was done in order to measure the residual enthalpy of the process and to obtain a fully crystalline sample which can then be considered inert at the temperature of the isotherm.
- Fifth, the sample was cooled down and stabilized again.
- And sixth, first and second steps were repeated with the inert fully crystallized sample. The new isothermal signal will be used as a baseline and compared with that obtained in the second step.

Transmission electron microscopy observations were performed on a Philips CM20 operating at 200 kV.

4. Results

4.1 Baseline and transitory effects

[Insert Figure 1 about here]

Isothermal signals obtained at different temperatures for as-cast and fully crystallized samples, respectively, are shown in figure 1. The inset shows the signal for times below 30 s. A huge peak (at short times after the annealing temperature is reached) is generally found for all the samples, independently of the isothermal temperature and the

Philosophical Magazine. Vol. 87. Núm. 27. 2007. Pag. 4151-4167
http://dx.doi.org/10.1080/14786430701530990
microstructural state of the sample. This peak can be ascribed to transitory effects of the equipment due to the change from non-isothermal to isothermal regime in the data acquisition. The fully crystalline sample can be considered as an inert sample at the isothermal annealing temperature; however, the signal is not a horizontal line but shows some drift even at long times, which can be ascribed to the equipment and depends on the specific conditions of the experiment (e.g. the mass of the sample) and slightly evolves for very long times (in the time order of days). This signal will be considered as a baseline for the corresponding signal obtained in the previous isotherm in the same DSC run. In our experiment, the separation in time between the acquisitions of the two isotherms is minimized as the experiments run without interruption. Another possibility to obtain a baseline would be to perform an isotherm without any sample. However, if the mass of the sample changes, its thermal inertia would be affected and, therefore, the present procedure of baseline acquisition is considered a better approach. In particular, once the signal is represented in power/mass units, the magnitude, shape and time position of the huge peak below 15 s is constant for different samples. The very good reproducibility of this maximum between the signal registered for one sample during the first (as-cast sample) and second (fully crystalline sample) isotherms enables the subtraction of the baseline to obtain an isothermal signal free from transitory effects for every temperature. The resulting curves are shown in figure 2.

[Insert Figure 2 about here]

Finally, it is worth noting the shift of the initial *dH/dt* value of the signal for the isotherm of the as-cast sample with respect to that of the fully crystalline one. This shift is a measure of the transformation rate at which the isotherm starts. This can be clearly observed in figure 3, where the shift $\Delta(dH/dt)$ is represented as a function of the isothermal temperature and along with the *dH/dt* DSC signal registered for an as-cast

Philosophical Magazine. Vol. 87. Núm. 27. 2007. Pag. 4151-4167
http://dx.doi.org/10.1080/14786430701530990
sample at 20 K/min, which was the heating rate used to reach the isothermal temperature.

[Insert Figure 3 about here]

The registered signal, *dH/dt*, can be linked with the transformation rate, *dX/dt*. The simplest way is to assume a relationship of proportionality between the enthalpy and the fraction of the nanocrystallization process. Although the validity of this assertion has been questioned, especially for the final stages of the process [23], it can be considered a fairly good approximation, widely used for both isothermal and non-isothermal kinetic analyses.

4.2 Information extracted from non-isothermal scans

It has been shown that the isothermal annealing below the onset temperature of the nanocrystallization, T_o, is not able to complete, in a reasonable time, the nanocrystallization process but a residual exothermic peak remains even for very long annealing times [7,24,25]. Consequently, the total fraction of transformation (normalized to 1) can not be obtained directly from the enthalpy released in the isotherm, because the process is only partially completed during this treatment. Therefore, in order to complete the nanocrystallization process, a non-isothermal DSC scan must be used.

[Insert Figure 4 about here]

The total enthalpy involved in the nanocrystallization process of an as-cast sample heated at 20 K/min can be used to normalize the fraction of the nanocrystallization process. However, as it can be seen in figure 3, a small overlapping

Philosophical Magazine. Vol. 87. Núm. 27. 2007. Pag. 4151-4167
http://dx.doi.org/10.1080/14786430701530990
between the nanocrystallization process and the second transformation stage occurs for the studied composition. In order to properly measure the value of the enthalpy of the whole nanocrystallization process, the enthalpy of the second peak must be subtracted from the enthalpy of both overlapped peaks. Figure 4(a) shows the DSC scans at 20 K/min performed after each isothermal treatment. The scan of the as-cast sample is also shown. It can be observed that the second DSC peak is not altered by any isothermal annealing performed in this study. The integration of each DSC signal taken at 20 K/min generally shows a two step increase of the absolute value of the enthalpy corresponding to the two processes detected, except for the non-isothermal scan performed after the isotherm at 853 K, indicating that the nanocrystallization is practically finished after this isotherm and only the second exotherm is detected (see Fig. 4(a)). Therefore, the integration curve of the DSC scan after annealing at 853 K has been subtracted to all the others and the resulting values of enthalpy have been normalized taken into account that the final value corresponds to X=1 (completed nanocrystallization process). On the other hand, the initial X value depends on the isothermal annealing previously performed and can be calculated from the residual enthalpy, ΔH_{res}, under the DSC curves of Fig. 4(a) as $1-\Delta H_{res}/\Delta H_{Total}$. The resulting curves are plotted in figure 4(b). The curves collapse as expected for an isokinetic process.

Finally, it must be considered the value of the fraction of the nanocrystallization process completed before the isotherm, as some of the isotherms were performed at temperatures above the onset of the nanocrystallization process. This value can be clearly obtained from the integration curve of the DSC scan at 20 K/min of the as-cast sample, as this was the procedure followed to reach the isothermal temperature in every case.

Philosophical Magazine. Vol. 87. Núm. 27. 2007. Pag. 4151-4167
http://dx.doi.org/10.1080/14786430701530990

Summarizing, the isotherms involve a fraction of the transformation, *X(t,T),* from a initial value $X^{ISO}_{initial}(T) \geq 0$ (from the enthalpy released up to *T* measured from a 20 K/min DSC scan of the as-cast alloy) to a final value $X^{ISO}_{final}(T) \leq 1$, which can be obtained as 1-$X_{res}(T)$, where $X_{res}(T)$ is the fraction of the nanocrystallization process, measured from a DSC scan at 20 K/min performed after the isothermal annealing. Table 1 shows the values corresponding to the different isotherms performed.

[Insert Table 1 about here]

[Insert Figure 5 about here]

The value of $X^{ISO}(T) = X^{ISO}_{final} - X^{ISO}_{initial}$ could be, a priori, also approached from the area below the DSC isothermal signal. Figure 5 shows a comparison between the ΔH^{ISO} values directly measured from the isotherms and the values calculated from non-isothermal runs as: $\Delta H^{ISO}_{calc} = \Delta H_{total} - \Delta H_{initial} - \Delta H_{res}$, where ΔH_{total} is the total enthalpy of the nanocrystallization process, $\Delta H_{initial}$ is the enthalpy of the process completed before the onset of the isotherm and ΔH_{res} is the enthalpy of the residual peak detected in the DSC scan at 20 K/min after the isotherm. A linear relationship can be observed but $\Delta H^{ISO}_{calc} > \Delta H^{ISO}$ in all cases. The specific heat must contribute to the non-isothermal DSC signal and not to the isothermal one, but this fact can not explain the difference found. The process studied is exothermic and the specific heat contribution is endothermic; therefore, it would even increase the observed difference. In fact, the problem arises due to intrinsic errors in measuring the area under the isothermal DSC curve. Although the integration has been extended up to the time at which the isothermal plot reaches a saturation value, some process could occur at the long tails of the isothermal scans being so weak and extended in time that the deviation from the baseline could not be conveniently observed but jeopardized by the effects of baseline

Philosophical Magazine. Vol. 87. Núm. 27. 2007. Pag. 4151-4167
http://dx.doi.org/10.1080/14786430701530990

drifts (not completely avoided after baseline subtraction) and the resolution of the equipment (~ ± 0.005 W/g, which is larger than the shift of the baseline necessary to compensate the difference between ΔH_{calc}^{ISO} and ΔH^{ISO}, ~0.002 W/g for a 5 h isotherm). In order to estimate the relative importance of the enthalpy developed at the tails of the isotherms, some of them were repeated but only up to 2000 s. Figure 6 shows the residual non-isothermal DSC exotherms after 2000 s and 18000 s annealing along with the DSC signal of the as-cast sample for two different temperatures. No significant difference can be observed for the isotherm at 743 K, indicating that the transformation enthalpy between 2000 and 18000 s can be neglected. However, the isotherms performed at 813 K, which start with ~50 % of the process completed, show 77 % and 81 % of completion of the nanocrystallization process for annealing times of 2000 and 18000 s, respectively. It is worth noting that, at this temperature, the process is slowed down as it corresponds to the long tails of the DSC signal observed at the final stages of the nanocrystallization (low values of the transformation rate). The difference found in ΔH between both 813 K experiments is only of 6 J/g and a shift of the baseline of only 0.0003 W/g (one order of magnitude lower than the resolution of the equipment) could account for this difference extending the integration up to 18000 s. All these intrinsic problems in the analysis of the isothermal signals yield a more accurate approach to use non-isothermal experiments for measuring the enthalpies. Although, for non-isothermal scans, the error in *dH/dt* is the same, data are acquired in a significantly shorter time thus the relative error is much smaller. Moreover, the enthalpy values must be normalized to the value of the total enthalpy involved in the nanocrystallization process and this value can only be measured from a non-isothermal experiment; therefore, the X^{ISO} values used were those calculated from non-isothermal runs. The fact that the contribution of the specific heat to the heat flow might be considered in non-isothermal

Philosophical Magazine. Vol. 87. Núm. 27. 2007. Pag. 4151-4167
http://dx.doi.org/10.1080/14786430701530990

regimes and can be ignored for isothermal ones is not affecting the calculations as the only values used to normalize the data were extracted from non-isothermal scans.

[Insert Figure 6 about here]

5. Discussion

Following Eqs. 4 and 8, the JMAK and AR plots are shown in figure 7. The values t_0=85 and 54 s were measured for the isotherms at T^{ISO}=743 and 753 K, respectively ($T^{ISO}<T_o$=769 K, nanocrystallization onset temperature at 20 K/min) and t_0=0 s was imposed for the isotherms performed at temperatures above T_o considering an initial value of $X(0)\neq 0$ (the process is already started). No much difference can be observed between both theories. The JMAK plot of the isotherm below T_o roughly exhibits two slopes and although, in some cases, AR theory can fit this kind of two-slope JMAK plots with a single straight line [5] this result is not achieved in the present case.

[Insert Figure 7 about here]

A further discussion can be done calculating the local values $n(X)$ and $n^*(X)$ (JMAK and AR theories, respectively). Figure 8 shows the local values of the two exponents for different isotherms and compared with the values obtained from a non-isothermal scan at 20 K/min. While isothermal regimes supply values of n and n^* in a certain range of X, from $X^{ISO}_{initial}$ to X^{ISO}_{final}, non-isothermal regimes (using the approach described on [21] for JMAK theory and extended to AR theory in the present work) are able to give a general view of the process from X=0 to 1. A good agreement can be found, supporting the isokinetic behaviour of the nanocrystallization of the $Fe_{60}Co_{18}Nb_6B_{16}$ alloy described from the study of the process at different heating rates [21], independently of the theory employed (JMAK or AR). No big differences can be

found between the results obtained by both theories and the use of the expression (2) would not support any extra result as the values must lay between the two limit cases studied: $0<\gamma<1$.

[Insert Figure 8 about here]

The value of the Avrami exponent is ~1-1.5 at the early stages of nanocrystallization and decreases below 0.5 as the nanocrystallization progresses. These values are in agreement with those obtained from thermomagnetic gravimetry [26] and other non-isothermal approaches as Gao-Wang and Ozawa methods [16,21]. The decrease of n as X increases has also been observed for the nanocrystallization process of other alloys (e.g. [27,28]). However, values of n below 1.5 (which theoretically should indicate no nucleation and three dimensional diffusion controlled growth [6]) have no sense in the JMAK theory considering growing crystallites. In this theory, for three dimensional growth, $n=n_i+3n_g$, where n_i refers to nucleation (1 if it is constant and 0 if it is absent) and n_g refers to growth (1 if it is interface controlled and ½ if it is diffusion controlled). Although AR theory accounts for another impingement factors besides the geometrical one, the values of n^* are still too low to give more than just a qualitative interpretation of a possible strongly hindered growth process, increasing the impingement as the crystalline volume fraction increases. However, as it will be shown below for the studied alloy, Avrami exponent below 1 could be also interpreted if the growth process is neglected after assuming an instantaneous growth approximation. In this case, $n=n_i$.

[Insert Figure 9 about here]

In the case of JMAK theory, the use of equation (3) (or Eq. (7) in the case of AR theory) implies some assumptions on the transformation kinetics. However, it has been shown that nanocrystallization process of FINEMET alloys can be described if a

derived form of JMAK equation is used (Eq. (1)) [15]. In this sense, some approximations can be done to simplify the calculations if the nanocrystalline microstructure developed is taken into account. Figure 9 shows a bright field transmission electron microscopy image of a nanocrystalline sample of the studied composition. Unlike FINEMET [24,29] and FeCoNbBCu alloys [30], which can be characterized by regularly shaped nanocrystals, the studied alloy shows very irregular crystallites which can be described as an agglomeration of orientationally related smaller ones (~5 nm in diameter). This is evidenced in figure 4 of reference [30] from the comparison of a bright and a dark field image of the same nanocrystal. A similar microstructure has also been observed in Cu-free NANOPERM alloys [3] and Zr-containing HITPERM alloys [31].

This microstructure has been qualitatively explained as resulting from a competition between two different nucleation phenomena and a strongly hindered growth process [32], which constraints the maximum size of the small crystalline units to 5 nm. The two nucleation phenomena correspond to the formation of nuclei in either isolated regions or in contact with a previously formed nanocrystal. The former mechanism has the advantage of a richer Fe content in the surroundings as the region is far from other nanocrystals and not depleted in Fe. The latter mechanism has the advantage of a reduced interface energy. Therefore, a possible approximation of the nanocrystallization kinetics of the studied alloy could be to consider an instantaneous growth of the small crystalline units up to their maximum size (~5 nm in diameter). It is worth mentioning that the second mechanism cannot exist since the very beginning of the crystallization process, as it needs the presence of crystallites. This could explain the n values above 1, which would indicate an increasing nucleation rate at the early stages of the nanocrystallization.

Philosophical Magazine. Vol. 87. Núm. 27. 2007. Pag. 4151-4167
http://dx.doi.org/10.1080/14786430701530990

Assuming an instantaneous growth in equation (12) of reference [15], the extended transformed volume fraction can be written as:

$$X^{ext} = \frac{1}{x_C}\frac{\pi < d >^3}{6}\int_0^t I(\tau)d\tau + X^{ext}(0) \tag{10}$$

where x_C is the crystalline volume fraction at the end of the nanocrystallization process (~0.54), $<d>$ is the average size of the small spherical crystalline units forming the agglomerates and I is the nucleation frequency. Combining equation (1) and (10) it is possible to obtain the nucleation frequency as:

$$I(X,T) = \frac{6x_C}{\pi < d >^3}\frac{1}{1-X}\frac{dX}{dt}(T) \tag{11}$$

The resulting curves are plotted in figure 10. The X dependence of the $I(X,T)$ curves can be interpreted in the frame of the above described hypothesis of two nucleation processes: At the beginning of the nanocrystallization, the only possible process is the formation of isolated nuclei. As these nuclei are formed, the second nucleation process can occur and, therefore, the nucleation frequency increases. As the nanocrystallization progresses, the depletion of Fe content in the amorphous matrix affects both nucleation mechanisms and the nucleation frequency decreases for high crystalline volume fraction.

[Insert Figure 10 about here]

In order to explore the thermal dependence of the nucleation frequency, an Arrhenius functional form has been proposed and for fixed values of X, $\ln[I]$ vs $1/T^{ISO}$ plots have been fitted to straight lines:

$$\ln[I] = \ln[A] - \frac{Q}{RT} \tag{12}$$

The Q values obtained, 2.5-6 eV, are of the order of those obtained from different experiments [16,21,26]. Besides the experimental errors, other factors could

Philosophical Magazine. Vol. 87. Núm. 27. 2007. Pag. 4151-4167
http://dx.doi.org/10.1080/14786430701530990

explain the differences observed between the activation energies obtained from different approaches and techniques. Non-isothermal approaches [16,21] supply averages values of Q. On the other hand, it has been shown that the superparamagnetic behaviour exhibited by the studied alloy at the very early stages of crystallization provokes an important magnetic field dependence of the crystallization onset detected by thermomagnetic techniques [33]. Figure 11 shows the X dependence found for ln[A] and Q. A linear relationship has been found between these two parameters as it is also represented in Fig. 11:

$$\ln[A] = -15.3(9) + 16.1(2)Q \quad (13)$$

This linearity has been previously reported in the devitrification of amorphous alloys [34], ascribed to the presence of a distribution of microprocesses during devitrification [35]. Combining equations (12) and (13) it is possible to obtain a phenomenological expression for the nucleation frequency during the nanocrystallization process of the $Fe_{60}Co_{18}Nb_6B_{16}$ alloy as:

$$I(X,T) = I_0 \exp\left[\frac{Q(X)}{R\theta}\frac{T-\theta}{T}\right] \quad (14)$$

where θ=721±9 K and I_0~$2\cdot10^{-7}$ $s^{-1}nm^{-3}$ (with an error of the order of 10^{-7} $s^{-1}nm^{-3}$).

[Insert Figure 11 about here]

There is a change in the behaviour of ln[A] and ln[Q] for X>0.5, being constant. This change can be also observed in the local Avrami exponent, which reaches an almost constant value for high crystallization fractions (see Fig. 8). This change could be ascribed to a change in the nucleation mechanisms.

Conclusions

Philosophical Magazine. Vol. 87. Núm. 27. 2007. Pag. 4151-4167
http://dx.doi.org/10.1080/14786430701530990

A procedure to optimize the information obtained from isothermal transformation of metastable systems has been proposed and applied to the nanocrystallization process of an amorphous metallic alloy.

Nanocrystallization enthalpy information has been extracted from isothermal DSC scans after subtracting a baseline which resembles the transitory effects due to the equipment and using enthalpy values obtained from non-isothermal scans performed before and after the isotherm. In order to normalize the nanocrystallization fraction to the value at the end of the process it is necessary to use non-isothermal scans, as isotherms, if the nanocrystallization process would be completed, it would require a very long time. Moreover, the measurement of enthalpies in non-isothermal scans is more accurate as the integration range is smaller.

Results have been studied in the frame of Johnson-Mehl-Avrami-Kolmogorov and Austin-Rickett theories. Good agreement has been found between isothermal and non-isothermal kinetics, supporting the isokinetic character of the nanocrystallization process studied. The n and n^* values are too low and can not be discussed in the frame of these theories, although a qualitative interpretation can be given after TEM observations of the very small units (~5 nm diameter) forming the crystalline agglomerates: nucleation process is constant at the beginning of the process and progressively decreases as nanocrystallization progresses. This would yield, neglecting the growth process, an Avrami exponent of ~1 for low crystalline volume fraction, decreasing at higher values of X. In this sense, a very simple model based on instantaneous growth of these very small units was used to obtain a phenomenological dependence of the nucleation frequency with the crystalline volume fraction and the temperature.

Philosophical Magazine. Vol. 87. Núm. 27. 2007. Pag. 4151-4167
http://dx.doi.org/10.1080/14786430701530990

Acknowledgments

This work was supported by the Spanish Government and EU FEDER (Project MAT 2004-04618) and by the PAI of the Regional Government of Andalucía (Spain). J.S.B. acknowledges a research contract from this Regional Government.

Philosophical Magazine. Vol. 87. Núm. 27. 2007. Pag. 4151-4167
http://dx.doi.org/10.1080/14786430701530990

References

[1] M. E. McHenry, M. A. Willard, D. E. Laughlin, Prog. Mater. Sci. **44** 291 (1999).
[2] A. Inoue, Prog. Mater. Sci. **43** 365 (1998).
[3] K. Suzuki, M. Kikuchi, A. Makino, A. Inoue, T. Masumoto, Mat. Trans. JIM **32** 961 (1991).
[4] Y. Zhang, P. J. Warren, A. Cerezo, Mat. Sci. Eng. A **327** 109 (2002).
[5] J. Burke in: The Kinetics of Phase Transformation in Metals, Pergamon Press, Oxford, 1965, p. 49.
[6] J. W. Christian, in: The Theory of Transformations in Metals and Alloys, Part 1, Pergamon Press, Oxford, 1975, p. 542
[7] E. Illekova, Therm. Acta **387** 47 (2002).
[8] V. Ocelik, K. Csach, A. Kasardova, J. Miskuf, P. Svec, K. kristiakova, I. Mat'ko, Scripta Mater. **35** 1301 (1996).
[9] C. F. Conde, A. Conde, Mater. Letters **21** 409 (1994).
[10] W. A. Johnson, R. F. Mehl, Trans. Am. Inst. Mining Met. Engrs. **135** 416 (1939).
[11] M. Avrami, J. Chem. Phys. **7** 1103 (1939).
[12] M. Avrami, J. Chem. Phys. **8** 212 (1940).
[13] M. Avrami, J. Chem. Phys. **9** 177 (1941).
[14] A. N. Kolmogorov, Bull. Acad. Sci. USSR, Phys. Ser. **1** 355 (1937).
[15] M. T. Clavaguera-Mora, N. Clavaguera, D. Crespo, T. Pradell, Prog. Mat. Sci. **47** 559 (2002).
[16] J. S. Blázquez, C. F. Conde, A. Conde, J. Non-Cryst. Solids **287** 187 (2001).
[17] P. Bruna, D. Crespo, R. González-Cinca, E. Pineda, J. Appl. Phys. **100** 054907 (2006).
[18] A. R. Yavari, D. Negri, Nanostruct. Mater. **8** 969 (1997).
[19] T. Tagami, S. I. Tanaka, J. Mat. Sci. **34** 355(1999).
[20] M. J. Starink, J. Mat. Sci. **36** 4433 (2001).
[21] J. S. Blázquez, C. F. Conde, A. Conde, Acta Mater. **53** 2305 (2005).
[22] J. B. Austin, R. L. Rickett, Trans. Am. Inst. Mining Met. Engrs. **135** 396 (1939).
[23] J. M. Barandiarán, I. Tellería, J. S. Garitaonandía, H. A. Davies, J. Non-Cryst Solids **329** 57 (2003).
[24] C. F. Conde, A. Conde, Mat. Sci. Forum **179-181** 581 (1995).
[25] E. Illekova, K. Czomorova, F. A. Kuhnast, J. M. Fiorani, Mat. Sci. Eng. A **205** 166 (1996).
[26] J. S. Blázquez, C. F. Conde, A. Conde, Appl. Phys. A **76** 571 (2003).
[27] G. A. Jones, P. Bonnett, S. F. H. Parker, J. Magn. Magn. Mat. **58** 216 (1986).
[28] J. S. Blázquez, H. Dimitrov, J. Latuch, T. Kulik, Sol. State Phenom. **101-102** 265 (2005).
[29] M. Millán, C. F. Conde, A. Conde, J. Mat. Sci. **30** 3591 (1995).
[30] J. S. Blázquez, V. Franco, A. Conde, J. Phys.: Cond. Matter **14** 11717 (2002).
[31] D. H. Ping, Y. Q. Wu, K. Hono, M. A. Willard, M. E. McHenry, D. E. Laughlin, Scripta Mater. **45** 781 (2001).
[32] J. S. Blázquez, C. F. Conde, A. Conde, Arch. Mat. Sci **25** 407 (2004).
[33] J. S. Blázquez, V. Franco, C. F. Conde, A. Conde, S. Roth, J. Appl. Phys. **97** 044308 (2005).
[34] P. Svec, P. Duhaj, Phys. Stat. Sol (a) **105** 320 (1988).
[35] K. Kristiakova, P. Svec, Phys. Rev. B **64** 184202 (2001).

Philosophical Magazine. Vol. 87. Núm. 27. 2007. Pag. 4151-4167
http://dx.doi.org/10.1080/14786430701530990

Table 1

Fraction of the nanocrystallization process completed before, $X_{initial}^{ISO}$, after, X_{final}^{ISO}, and during the isothermal treatment calculated from non-isothermal scans.

Isothermal temperature (K)	$X_{initial}^{ISO}$	X_{final}^{ISO}	$X^{ISO} = X_{final}^{ISO} - X_{initial}^{ISO}$
743	0	0.59	0.59
753	0	0.65	0.65
763	~0	0.78	0.78
784	0.17	0.85	0.68
813	0.51	0.91	0.40
853	0.75	1	0.25

Philosophical Magazine. Vol. 87. Núm. 27. 2007. Pag. 4151-4167
http://dx.doi.org/10.1080/14786430701530990

Figure caption

Figure 1: Isothermal DSC scans for as-cast and fully crystalline samples performed at two temperatures.

Figure 2: Enthalpy rate, *dH/dt*, vs time plots obtained from isothermal DSC signals after baseline subtraction.

Figure 3: Difference between the initial values of the DSC isothermal signals for as-cast and fully crystalline samples (each point corresponds to a DSC experiment). A non-isothermal DSC scan at 20 K/min of the as-cast sample is also plotted for comparison.

Figure 4: (a) Enthalpy rate, *dH/dt*, obtained from non-isothermal scans and (b) nanocrystallization fraction, *X*, obtained for samples isothermally annealed 5 hours at different temperatures vs. temperature (The corresponding plots of the as-cast sample are also shown for comparison).

Figure 5: Enthalpy involved in the isothermal annealing (calculated from non-isothermal runs before and after the isotherm) as a function of the enthalpy directly measured from the isothermal scan.

Figure 6: Comparison between the as-cast and the residual DSC plots at 20 K/min after annealing for 2 and 18 ks at 743 and 813 K. Arrows indicate the temperature of the previous isotherm.

Figure 7: Austin-Rickett and Avrami plots: $\ln[1/(1-X)-1]$ and $\ln[-\ln(1-X)]$ vs. $\ln(t-t_0)$, respectively, for selected isothermal treatments. X is the nanocrystallization fraction, t the time and t_0 the induction time.

Figure 8: Local Avrami and Austin-Rickett exponents: $n(X)$ and $n^*(X)$, respectively, vs nanocrystallization fraction, X.

Figure 9: Bright field TEM image of a sample annealed 750 min at 716 K.

Philosophical Magazine. Vol. 87. Núm. 27. 2007. Pag. 4151-4167
http://dx.doi.org/10.1080/14786430701530990

Figure 10: Nucleation frequency, *I,* as a function of *X* for different isothermal annealing temperatures.

Figure 11: (a) ln[*A*] and *Q* as a function of *X*. (b) Linear dependence of ln[*A*] with *Q*.

Philosophical Magazine. Vol. 87. Núm. 27. 2007. Pag. 4151-4167
http://dx.doi.org/10.1080/14786430701530990

Figure 1

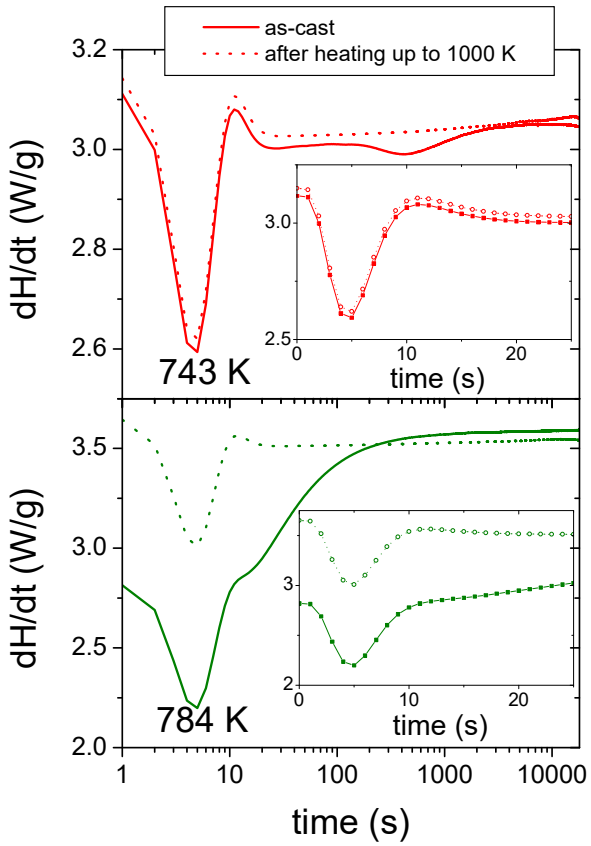

Philosophical Magazine. Vol. 87. Núm. 27. 2007. Pag. 4151-4167
http://dx.doi.org/10.1080/14786430701530990

Figure 2

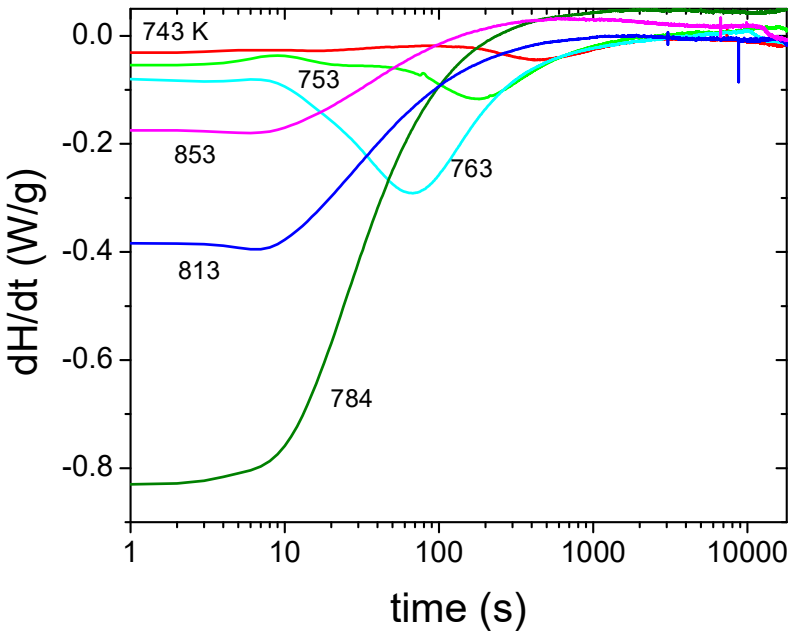

Philosophical Magazine. Vol. 87. Núm. 27. 2007. Pag. 4151-4167
http://dx.doi.org/10.1080/14786430701530990

Figure 3

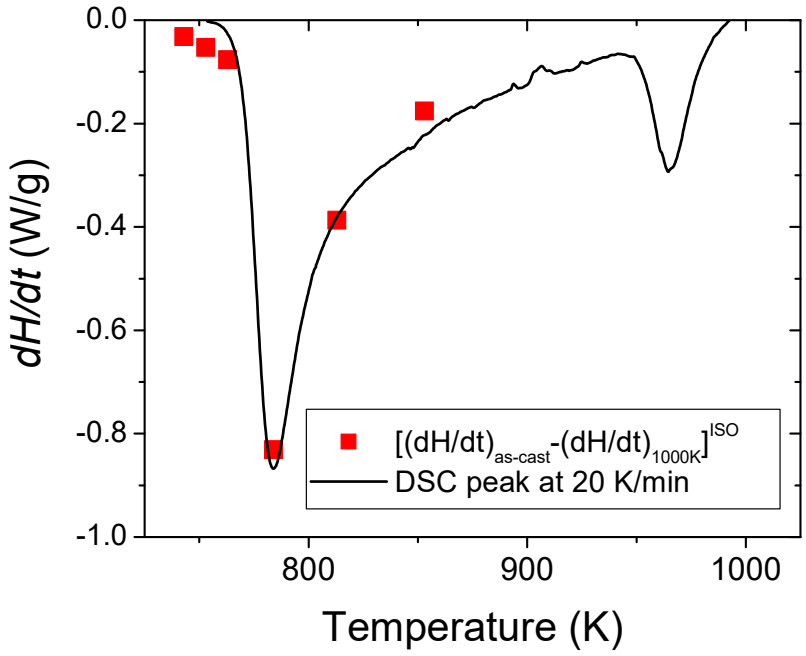

Philosophical Magazine. Vol. 87. Núm. 27. 2007. Pag. 4151-4167
http://dx.doi.org/10.1080/14786430701530990

Figure 4

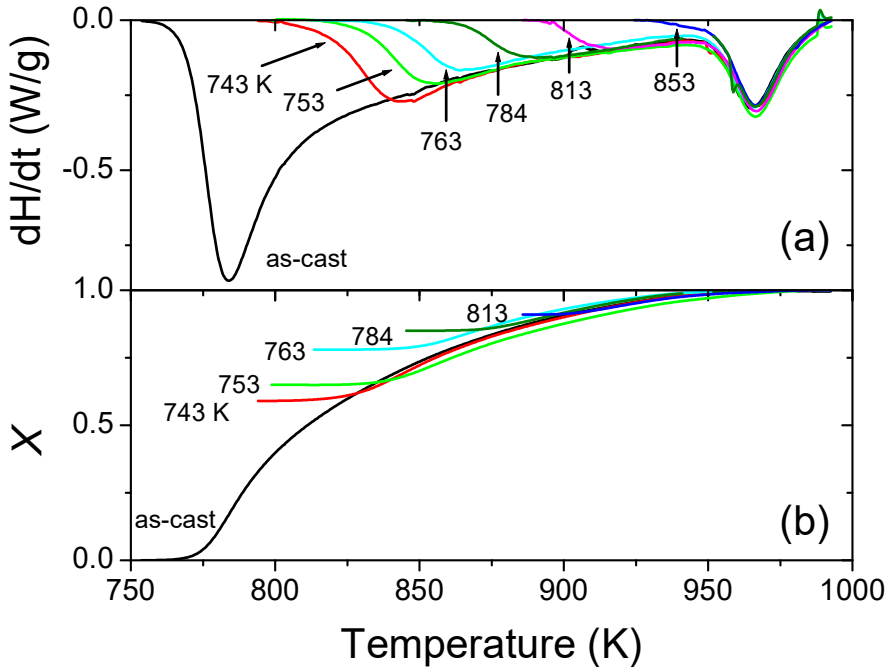

Philosophical Magazine. Vol. 87. Núm. 27. 2007. Pag. 4151-4167
http://dx.doi.org/10.1080/14786430701530990

Figure 5

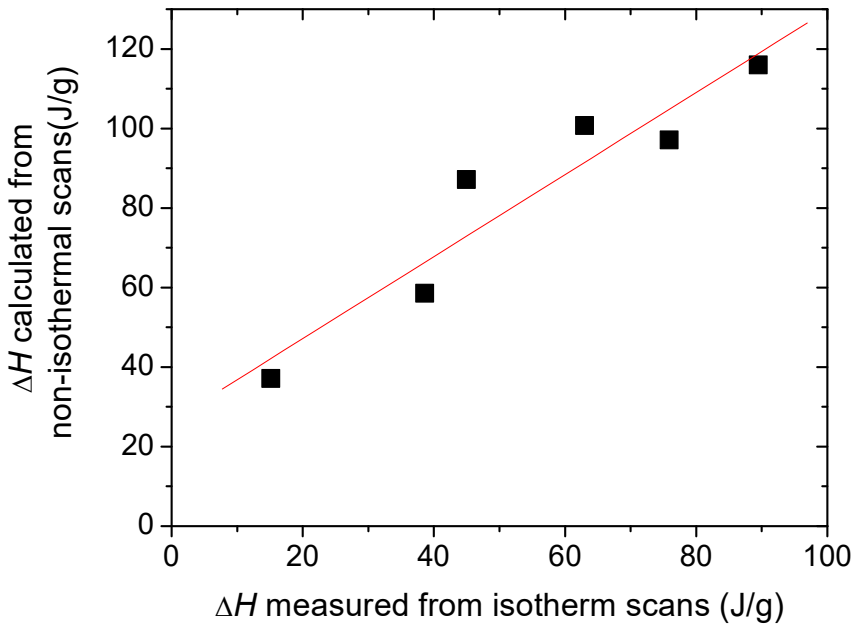

Philosophical Magazine. Vol. 87. Núm. 27. 2007. Pag. 4151-4167
http://dx.doi.org/10.1080/14786430701530990

Figure 6

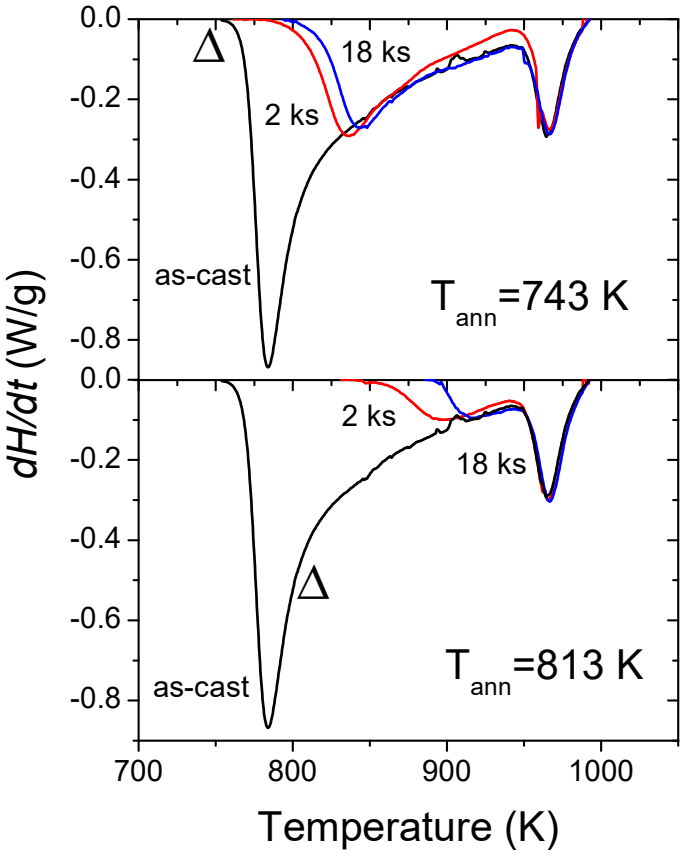

Philosophical Magazine. Vol. 87. Núm. 27. 2007. Pag. 4151-4167
http://dx.doi.org/10.1080/14786430701530990

Figure 7

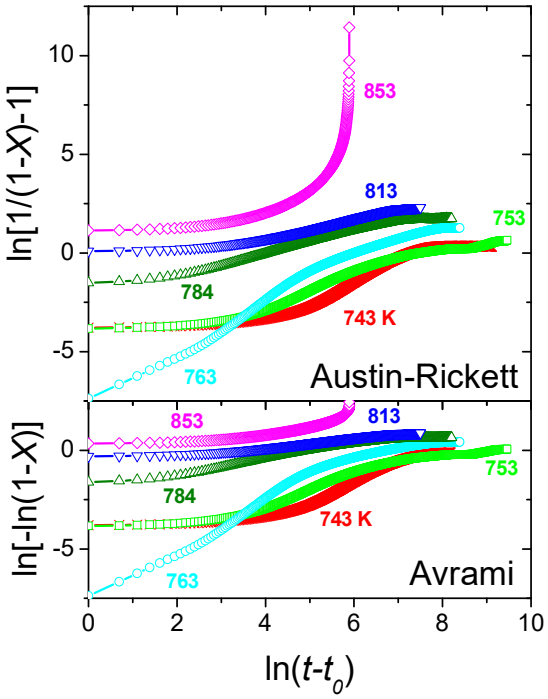

Philosophical Magazine. Vol. 87. Núm. 27. 2007. Pag. 4151-4167
http://dx.doi.org/10.1080/14786430701530990

Figure 8

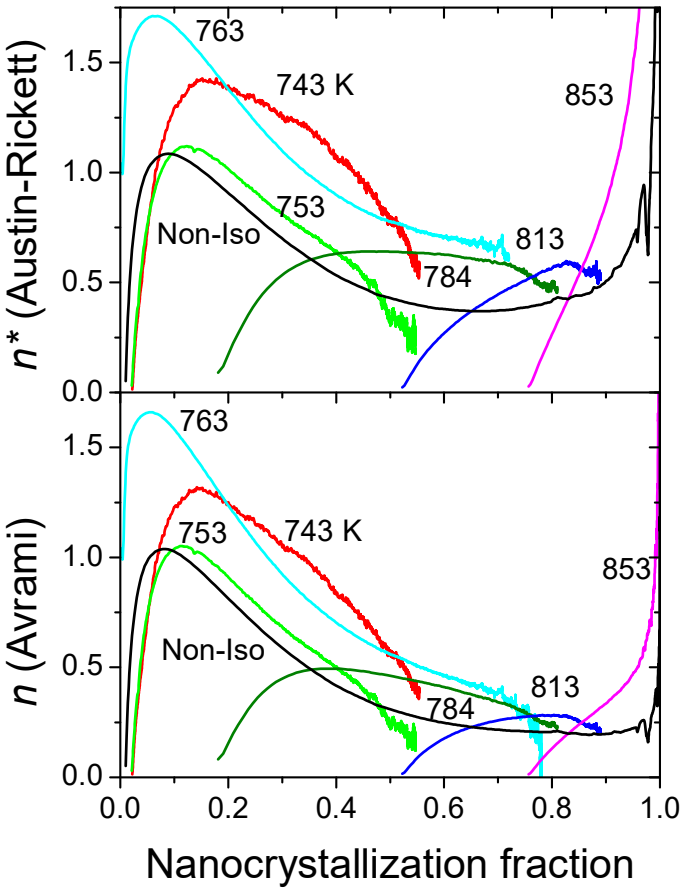

Philosophical Magazine. Vol. 87. Núm. 27. 2007. Pag. 4151-4167
http://dx.doi.org/10.1080/14786430701530990

Figure 9

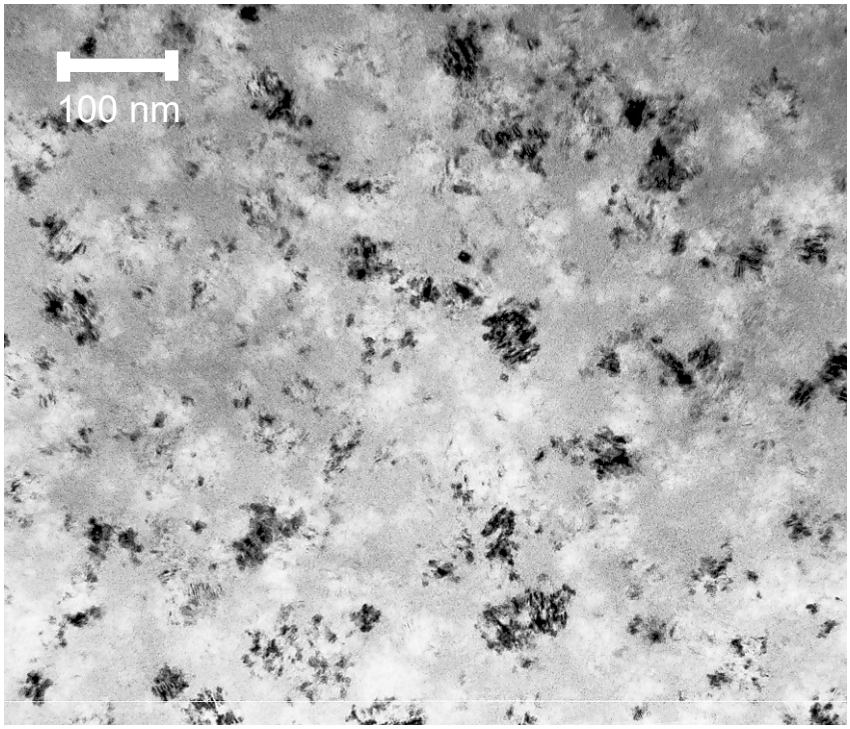

Philosophical Magazine. Vol. 87. Núm. 27. 2007. Pag. 4151-4167
http://dx.doi.org/10.1080/14786430701530990

Figure 10

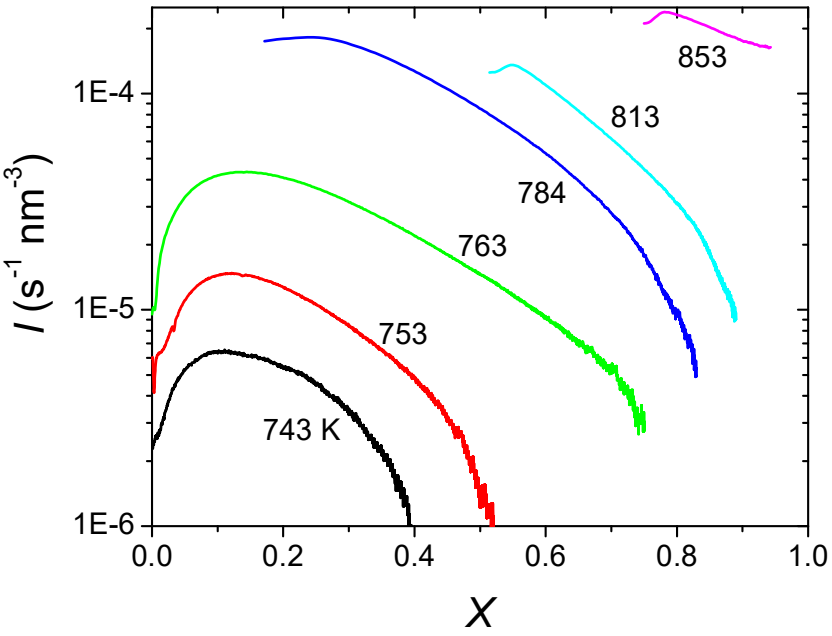

Philosophical Magazine. Vol. 87. Núm. 27. 2007. Pag. 4151-4167
http://dx.doi.org/10.1080/14786430701530990

Figure 11